# Magnetism and magneto-optical effects in bulk and few-layer $CrI_3$: A Theoretical GGA + *U* study

**VIJAY KUMAR GUDELLI**
**Physics Division**
**National Center for Theoretical Sciences**

# Outline of the talk:

- Facts and findings about the $CrI_3$ materials
- Magneto-optical (MO) properties
- Computational details
- Results and discussion
- Conclusion

# Facts and Findings about $CrI_3$:

- $CrI_3$ is polymorphic material
  - Monoclinic $AlCl_3$-type structure (SG: *C2/m*) at room temperature
  - Rhombohedral $BiI_3$-type structure (SG: *R-3*) below 240 K temperature

- Recent study confirms that rhombohedral (*R-3*) phase is the more stable than the monoclinic (*C2/m*) phase

- Cleavage energy of $CrI_3$ is 0.30 J/m$^2$, which is less than well-known graphite of (0.43 J/m$^2$) and $MoS_2$ of 0.27 J/m$^2$, confirms this material can be easily exfoliated as layered materials (which is evident from the experimental studies in the recent years)

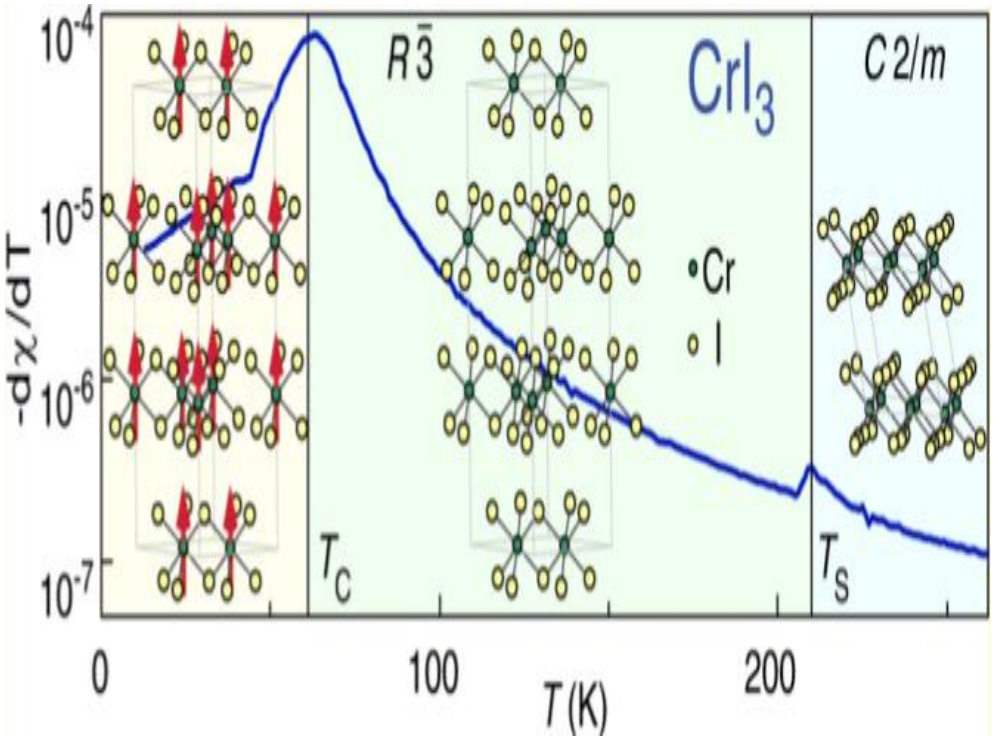


*McGuire et al., Chem. Mater. 27, 612 (2015)

# Facts and Findings about $CrI_3$:

- Bulk crystalline $CrI_3$ is a layered Ising ferromagnetic material below a Curie temperature ($T_C$) of 61 K with an out-of-plane easy axis*
- The van der Waals nature in bulk $CrI_3$ along with the magneto-crystalline anisotropy, the ferromagnetic nature is retained even in monolayer $CrI_3$#
- The observed monolayer $T_C$ of 45 K which is very close to the bulk Tc of 61 K, which suggests that the ferromagnetic monolayer of $CrI_3$ are weakly coupled to their substrates and can be regarded as isolated magnets #
- Recent study of Magneto-Optical Kerr-Effect (MOKE) in the layered ferromagnetic $CrI_3$ materials creates opportunities for studying magnetism in atomically thin materials, which finds application in spintronics and magneto-electronics devices

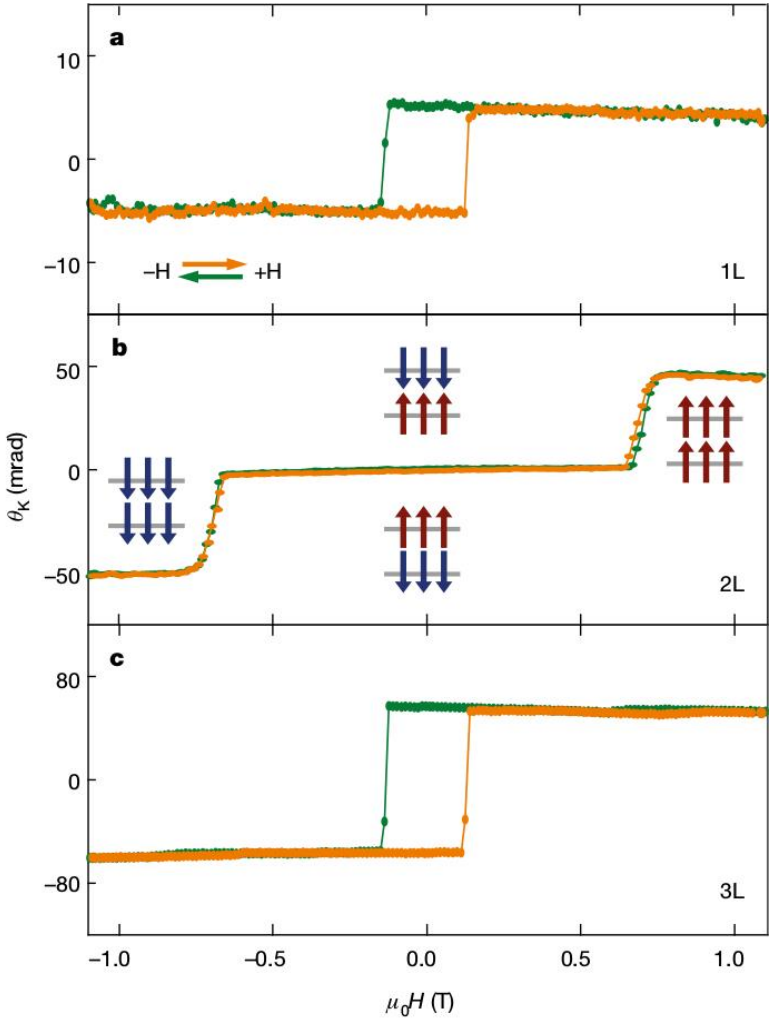


**Figure 3 | Layer-dependent magnetic ordering in atomically-thin $CrI_3$. a**, MOKE signal on a monolayer (1L) $CrI_3$ flake, showing hysteresis in the Kerr rotation as a function of applied magnetic field, indicative of ferromagnetic behaviour. **b**, MOKE signal from a bilayer $CrI_3$ showing vanishing Kerr rotation for applied fields ±0.65 T, suggesting antiferromagnetic behaviour. Insets depict bilayer (2L) magnetic ground states for different applied fields. **c**, MOKE signal on a trilayer (3L) flake, showing a return to ferromagnetic behaviour.

*Dillon et al, J. Appl. Phys. 36, 1259 (1965); McGuire et al, Chem. Mater. 27, 612–620 (2015)
#Huang et al, Nature, 546, 270, 2017 (figure);

# What are magneto-optical effects and how it will appear in magnetic materials?

# Relativistic (spin-orbit coupling induced) effects in magnetic solids:

- ✓ Orbital magnetization
- ✓ X-ray circular dichroism
- ✓ Perpendicular magneto-crystalline anisotropy in multilayers
- ✓ Joule (anisotropic) magnetostriction
- ✓ Magneto-electric coupling
- ✓ Magneto-optical effects (Faraday rotation and Kerr effect)

… … .

Fundamental cause: the simultaneous occurrence of electron spin-polarization and relativistic interaction (spin-orbit coupling) in the magnetic solids

# Magneto-optical properties:

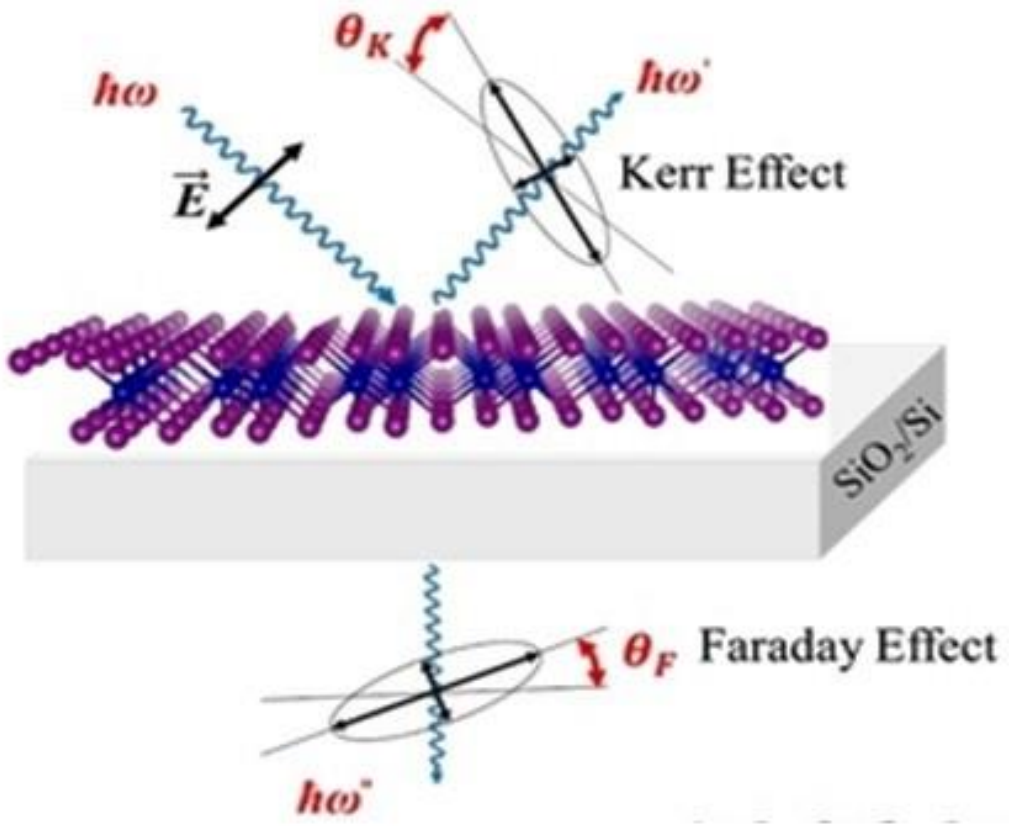


Faraday Effect (1845): The rotation of the polarization plane of linearly polarized light upon *transmission* through a magnetic material

Kerr Effect (1888): The rotation of the polarization plane of linearly polarized light upon *reflection* from the surface of a magnetic material

# How to get the Magneto-optical properties:

## Optical conductivity is the key ingredient for evaluating the magneto-optical properties

- The *absorptive parts* of the optical conductivity ($\sigma'_{xx}$ and $\sigma''_{xy}$) have direct physical interpretations of MO properties, i. e.,
- The *real diagonal* elements measures the average in absorptions of left- and right-circularly polarized lights

$$\sigma'_{xx}(\omega) = \frac{\lambda}{\omega}\sum_{k,jj'}^{n}\left[\left|\Pi^{+}_{jj'}\right|^2 + \left|\Pi^{-}_{jj'}\right|^2\right]\delta(\omega - \omega_{jj'})$$

- The *imaginary off-diagonal* elements is equal to the difference of left- and right-circularly polarized lights

$$\sigma''_{xy}(\omega) = \frac{\lambda}{\omega}\sum_{k,jj'}\left[\left|\Pi^{+}_{jj'}\right|^2 - \left|\Pi^{-}_{jj'}\right|^2\right]\delta(\omega - \omega_{jj'})$$

See here for more details: Feng *et al*, *2D Mater.* 4, 015017 (2017)

# How to get the Magneto-optical properties:

- The *dispersive parts* of the optical conductivity ($\sigma''_{xx}$ and $\sigma'_{xy}$) are calculated from absorptive parts using the Kramers-Kronig relation

- The *real diagonal* elements of dispersive is:

$$\sigma''_{xx}(\omega) = -\frac{2\omega}{\pi}\,\mathrm{P}\int_0^{\infty}\frac{\sigma'_{xx}(\omega')}{\omega'^2-\omega^2}\,\mathrm{d}\omega'$$

- The *imaginary off-diagonal* elements of dispersive is:

$$\sigma'_{xy}(\omega) = \frac{2}{\pi}\,\mathrm{P}\int_0^{\infty}\frac{\omega'\sigma''_{xy}(\omega')}{\omega'^2-\omega^2}\,\mathrm{d}\omega'$$

See here for more details: Feng *et al*, *2D Mater.* 4, 015017 (2017)

# How to get the Magneto-optical properties:

Kerr-effect: Complex polar Kerr angle for a magnetic thin-film, combining the rotation angle $\theta_K$ and ellipticity $\epsilon_K$, is written as

$$\theta_K + i\epsilon_K = i\frac{2\omega d}{c}\frac{\sigma_{xy}}{\sigma_{xx}^{s}}$$

$c$ is the speed of light in vacuum and

$\sigma_{xx}^{S}$ is the optical conductivity of a nonmagnetic substrate

Faraday-effect: The complex polar Faraday angle for a magnetic thin-film system is given by

$$\theta_F + i\epsilon_F = \frac{\omega d}{2c}(n_+ - n_-)$$

$n_+$ and $n_-$ represent the refractive indices for left- and right-handed polarized lights

$$n_{\pm}^2 = 1 + \frac{4\pi i}{\omega}(\sigma_{xx} \pm i\sigma_{xy})$$

See here for more details: Feng *et al*, *2D Mater.* 4, 015017 (2017)

# Computational Details:

- Projector augmented wave (PAW) method as implemented in the Vienna ab-initio simulation pack-age (VASP)
- Generalized gradient approximation of Perdew-Burke-Ernzerhof (PBE) parametrization is used for the exchange-correlation potential
- A plane-wave energy cut-off of 400 eV is used throughout the calculations
- K-mesh: 16 x 16 x 16 for bulk, 20 x 20 x 1 for layered structures
- To properly take into account of the Coulomb repulsion among the Cr *3d* electrons, we perform the *GGA + U* calculations which give a better description of the *3d* electron systems, with $U = 1\ eV$
- Fully relativistic projector augmented potentials are used to include the spin-orbit coupling

# Bulk

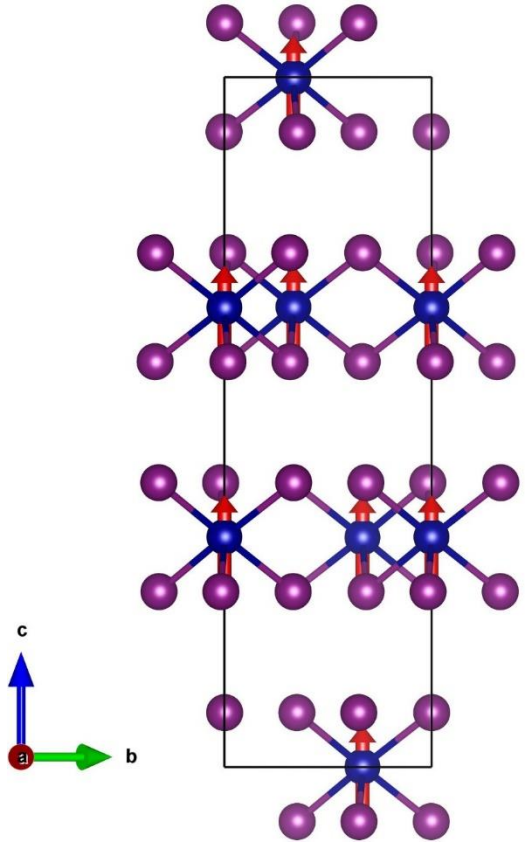


Bulk (conventional) $CrI_3$

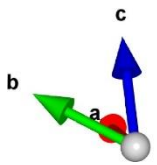


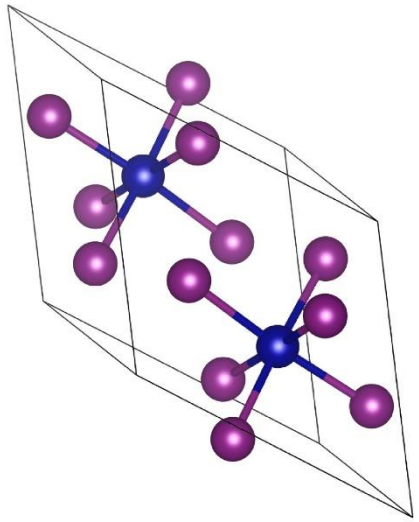

Bulk (primitive)

# Mono

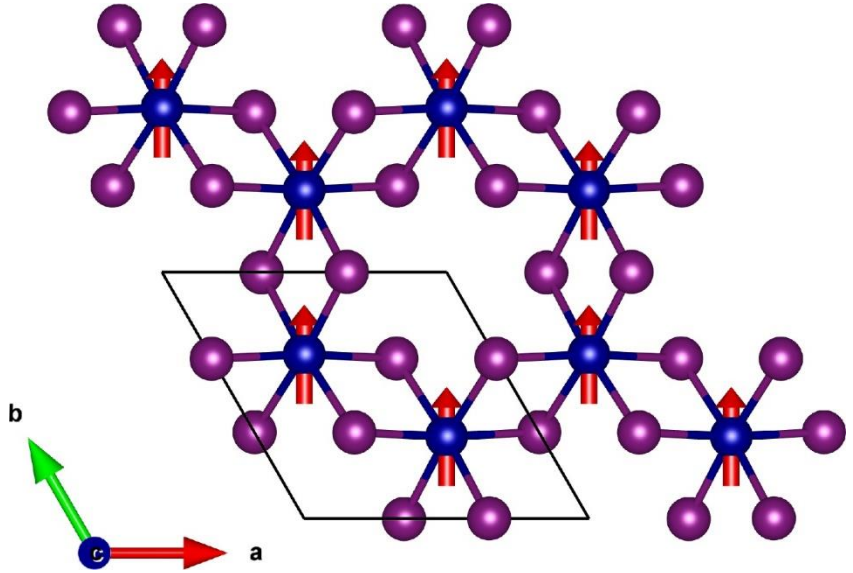


Mono layer (top view) $CrI_3$

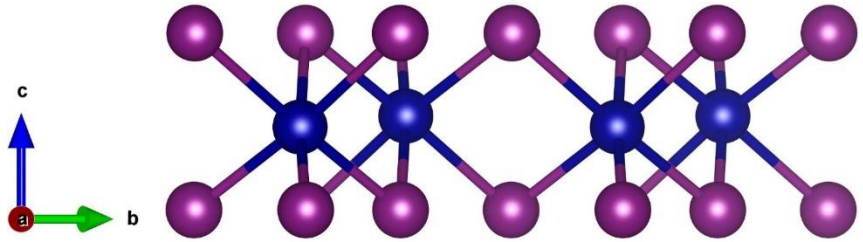


Mono layer (side view) $CrI_3$

# Effect of onsite Coulomb potential:

- We perform a series of the *GGA+U* calculations with the *U* value ranging from *0 to 3* eV for all the considered $CrI_3$ systems
- The calculated physical quantities (magnetic moment, magnetic anisotropy energy and band gap) do not depend significantly on the U value used
- This suggest that the results presented here remain more or less unchanged if a different U value were used

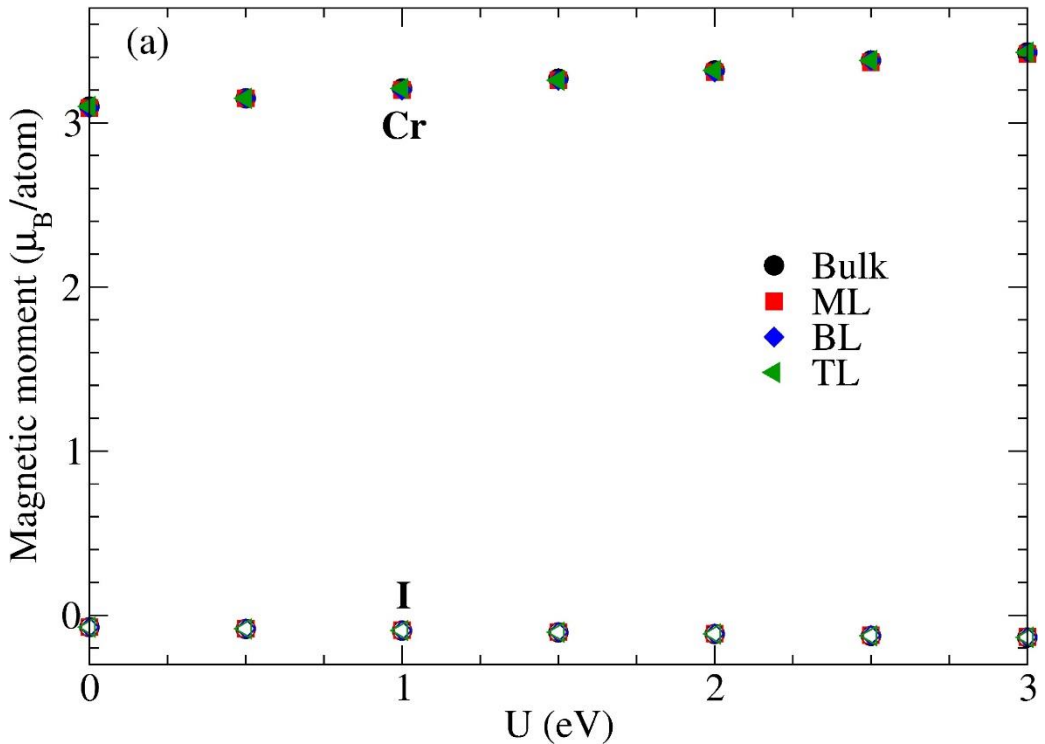


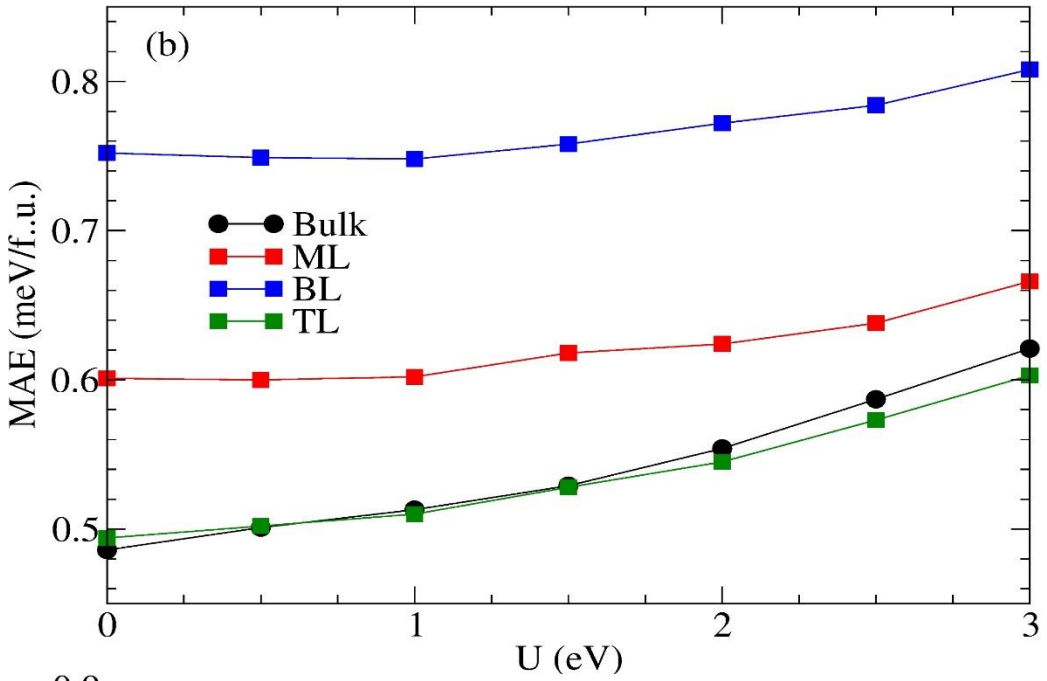


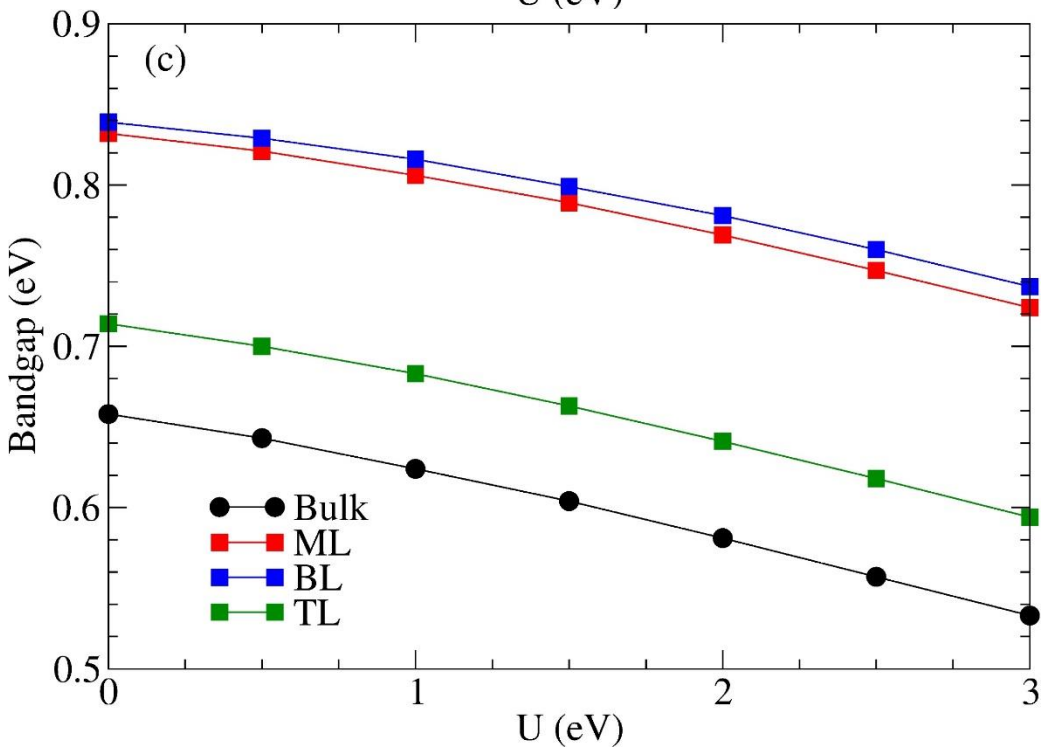

# Magnetic moment:

| | GGA+U (U = 1 eV) | |
|---|---|---|
| | Cr-Magnetic moment ($\mu_B$/fu) | I-Magnetic moment ($\mu_B$/fu) |
| Bulk | 3.20 (3.00*) | -0.094 |
| ML | 3.21 | -0.092 |
| BL | 3.21 | -0.094 |
| TL | 3.21 | -0.093 |

- The calculated spin magnetic moment of Cr of all the $CrI_3$ structures is about ~ 3.2 $\mu_B$, which is in good agreement with the experimental value of 3.0 $\mu_B$
- This is also consistent with three unpaired electrons in the Cr $t_{2g}$ configuration in these structures
- Interestingly, there is also a small induced magnetic moment (-0.09 $\mu_B$) on the I atom, which is antipallel to that of the Cr magnetic moment, in all the systems
- All these result in a total magnetic moment of 3.00 $\mu_B$/fu for all the structures

*McGuire et al., Chem. Mater. 27, 612 (2015)

# Magnetic exchange coupling constant (*J*):

- Among the magnetic properties of FM materials, magnetic ordering temperature ($T_c$) is very important quantity, to estimate the $T_c$ one need to calculate the exchange coupling constant (J)

- We calculated the exchange coupling parameters by mapping the total energies of different magnetic configurations with the classical Heisenberg Hamiltonian,

$$E = E_0 - \sum_{i,j} J_{ij}\, \hat{e}_i . \hat{e}_j$$

where, $E_0$ is the nonmagnetic ground state energy;
$J_{ij}$ is the exchange coupling parameter between sites i and j;
$\hat{e}_i$ the unit vector representing the direction of the magnetic moment on site *i*,

- The FM state is the most stable configuration for all the considered structures from the calculated total energies

- For the *intra exchange* mechanism in the $CrI_3$ structures, we have considered four intra layer magnetic configurations one FM, three antiferromagnetic (AF) structures, labelled as AF-Néel, AF-zigzag, and AF-stripe

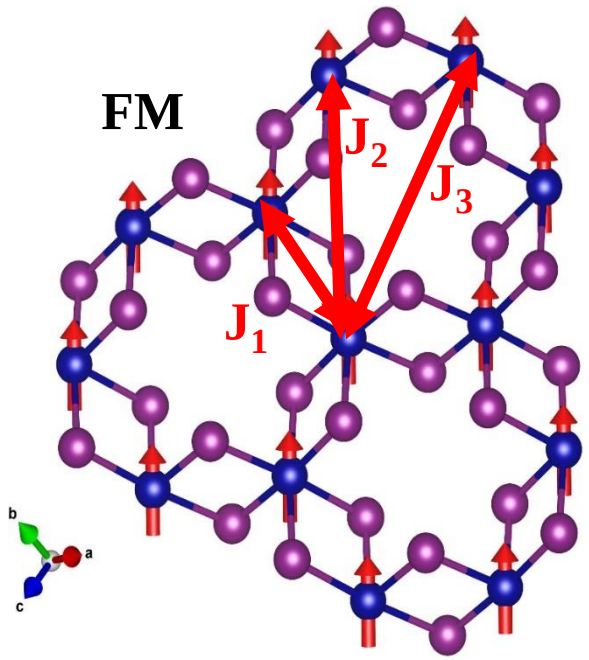


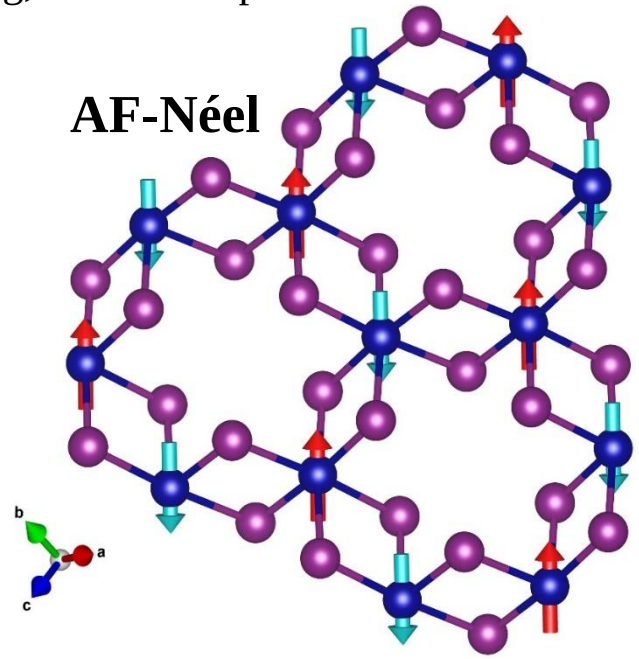


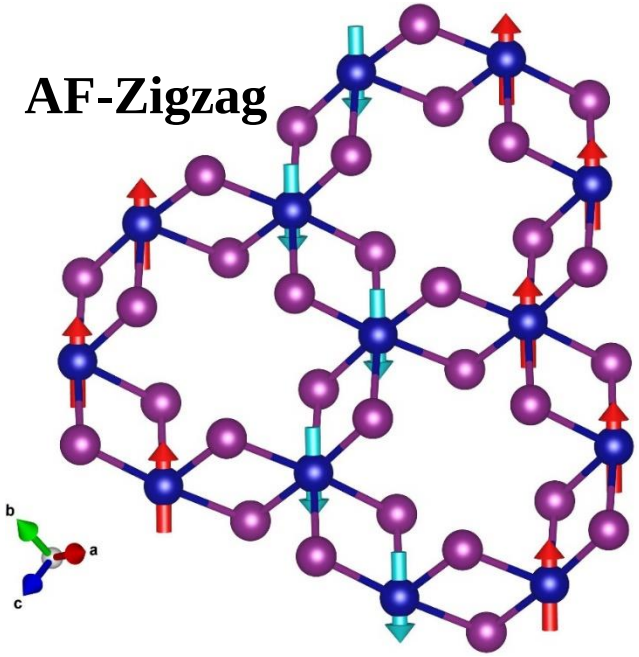


$$E = E_0 - \sum_{i,j} J_{ij}\, \hat{e}_i . \hat{e}_j$$

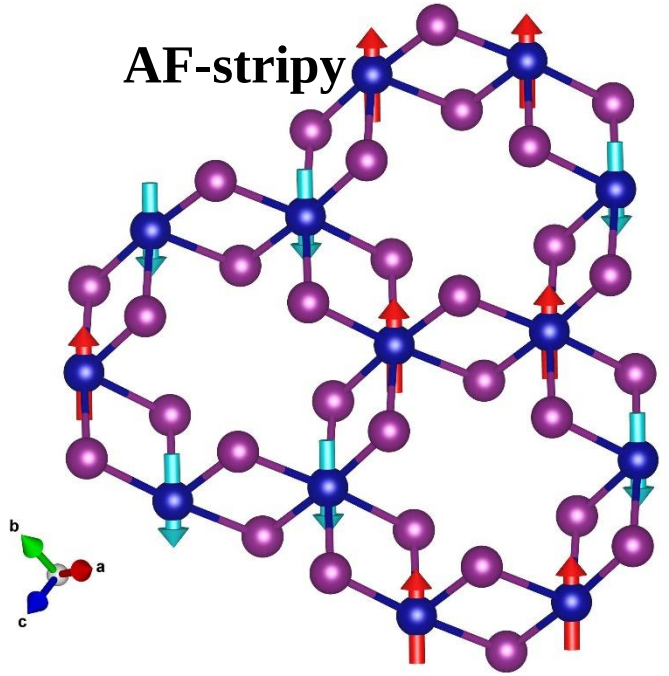


$$J_1 = \frac{-(E_{FM} - E_{AFM1} + E_{AFM2} - E_{AFM3})}{64}$$

$$J_2 = \frac{-(E_{FM} + E_{AFM1} - E_{AFM2} - E_{AFM3})}{128}$$

$$J_3 = \frac{-(E_{FM} - E_{AFM1} - 3E_{AFM2} + 3E_{AFM3})}{192}$$

$J_1$, $J_2$ and $J_3$ refereed as first-, second- and third-nearest neighbor interaction for all the considered materials

# Magnetic properties: Intra-layer exchange coupling

| Structures | $J_1$ (meV) | $J_2$ (meV) | $J_3$ (meV) |
|---|---|---|---|
| ML | 6.91 (6.4404) | 1.48 (1.4364) | -0.46 (-0.3447) |
| BL | 7.59 | 2.30 | 1.02 |
| TL | 8.05 | 2.45 | 0.91 |
| Bulk | 8.08 | 2.89 | 1.62 |

- The $J_1$ is positive, suggest a strong FM nature among the Cr-Cr in all the investigated structures, consistent with the total energies of FM stable state
- The $J_2$ is also FM (positive), the $J_2$ value is about 3.5 times smaller than $J_1$
- All the exchange interaction parameters are increasing monotonically with increasing the number of layers, which remark that the magnetic nature is strengthening as we move from ML to bulk via BL and TL

Jang et, al, JMCC, 3,12457 (2015)

# Magnetic properties: Inter-layer exchange coupling

| Structures | $J_z$ (meV) |
|---|---|
| BL | 2.97 |
| TL | 2.85 |
| Bulk | 2.95 |

- The calculated interlayer exchange coupling constant $J_z$ is also ferromagnetic for bulk, BL and TL structures
- This prediction agrees well with all previous experiments on all the structures except BL $CrI_3$ which has been found to be interlayer AFM
- All studies showed that the interlayer magnetic coupling in BL $CrI_3$ is strongly stacking dependent and is also sensitive to the exchange-correlation functional used
- GGA+U calculation with U=3 eV indicates that in the AB′-stacked BL $CrI_3$, the total energy of the AF configuration is slightly lower than that of the FM configuration (by merely~0.7 meV/unit cell), and this also confirmed by our own GGA+U calculations
- Clearly, further measurements on the stacking order in BL $CrI_3$ are needed to resolve this interesting problem

# Magnetic Anisotropic Energy (MAE):

- Magneto anisotropy energy is the total energy difference between the easy axis and hard axis magnetizations, i. e. $\Delta E_{MAE} = E_{100} \sim E_{001}$, which also refers as the energy require to flip the magnetization from easy axis to the hard axis direction

- MAE is particularly important for 2D magnetic materials

- According to the Mermin–Wagner theorem, a long-range magnetic order could not occur at any finite temperature in a 2D isotropic Heisenberg magnetic structure because of large thermal spin fluctuations

- However, this restriction can be lifted if the 2D system has a significant out-of-plane MAE, which suppress the thermal fluctuations and thus stabilize the long-range magnetic order at finite temperature

- For magnetic solids the MAE contributions arises mainly from two contributions

  (a) first one is from the magnetocrystalline anisotropy energy (MCE) ($\Delta E_b$) in the electronic band structure due to the simultaneous occurrence of the electron spin-orbit interaction and the spin polarization

  (b) Second one is from the magnetic dipolar anisotropy energy (MDE) ($\Delta E_d$) caused by the magnetostatic interaction in the magnetic solid

*Mermin et. at., Phys. Rev. Lett., 17,1133 (1966)
Tung et. at., Phys. Rev. B 76, 094413 (2007)

# Magnetic Anisotropic Energy (MAE (meV/FU)):

| Structures | MCE ($\Delta E_b$) | MDE ($\Delta E_d$) | $\Delta E_{MAE}$ |
|---|---|---|---|
| ML | 0.678 (0.686) | -0.152 | 0.526 |
| BL | 0.620 | -0.152 | 0.468 |
| TL | 0.586 | -0.152 | 0.434 |
| Bulk | 0.545 | -0.064 | 0.481 (0.26) |

- The MDE is *negative* prefers an *in-plane* magnetization, and the MCE is *positive* prefers the *out-of-plane* magnetization
- MDE < MCE, prefers the out-of-plane magnetization in all the systems
- The present obtained MAE of the ML $CrI_3$ structure is quantitatively in good agreement with the previously reported value of 0.686 meV/f.u.
- The calculated MAE of bulk $CrI_3$ agree reasonably well with the experimental reported value
- Interestingly, the MAEs of the $CrI_3$ multilayers are large and comparable to magnetic alloys such as FePt and CoPt
- The large MAEs could be attributed to two factors, namely, the quasi-2D structures of these materials and also the large SOC of the heavy ligand ion (I), these could have valuable applications in high density data storage devices

Gudelli et al, *New J. Phys.* **21** 053012 (2019)

# Magnetic properties: Transition temperature ($T_c$)

| Structures | $T_c^M$ (K) | $T_c^{SWT}$($T_c^{exp}$) (K) |
|---|---|---|
| ML | 109 | 66 (45) |
| BL | 165 | 69 |
| TL | 172 | 71 |
| Bulk | 191 | 73 (61) |

- $T_c$ within the mean-field approximation (MFA), i.e., $T_c^M = \frac{1}{3}\frac{J_0}{k_B}$, where $J_0 = 3J_1 + 6J_2 + 3J_3 + J_z$
- The estimated $T_c^M$ and measured $T_c$ agree in trend, i.e. the $T_c$ increases monotonically from ML, to BL, to TL and to bulk $CrI_3$
- However, $T_c^M$ is much higher compared to the experimental reports, the reason for this is, MFA neglects transverse spin fluctuations, which is especially strong in low-dimensional materials
- Furthermore, the MFA violates Mermin–Wagner theorem
- But, the out-of-plane MAE in 2D materials can establish long-range magnetic orders at finite temperatures by opening a gap in the spin wave spectrum which would suppress thermal spin fluctuations
- Based on the spin wave theory (SWT) with the out-of-plane MAE taken into account, $T_c = \frac{\pi J_1}{2\log(1+\frac{2\pi J_1}{\Delta_0})}$, where $\Delta_0$ is the spin wave gap, which can be roughly set to $\Delta_0 = \Delta E_{ma}$
- Compared with $T_c^M$, the $T_c^{SWT}$ values agree better with the corresponding experimental values

Gudelli et al, *New J. Phys.* **21** 053012 (2019)

# Band gap:

| | GGA+U (U = 1 eV) |
|---|---|
| | Band gap (eV) |
| Bulk | 0.62 (1.2[&]) |
| ML | 0.81 (0.91 with PBE 1.64eV with HSE)[#] |
| BL | 0.71 |
| TL | 0.68 |

- The calculated band gaps values of bulk $CrI_3$ is much smaller when compared to the experimental reported values
- The band gap increases slightly as bulk $CrI_3$ is thinned down to TL, to BL and finally to ML

[&]Dillon et al, J. Appl. Phys. 36, 1259 (1965)
[#] Jiang et. at., 1805.05675 (2018)

# Spin-polarised band-structure: $CrI_3$-Bulk and multi-layer

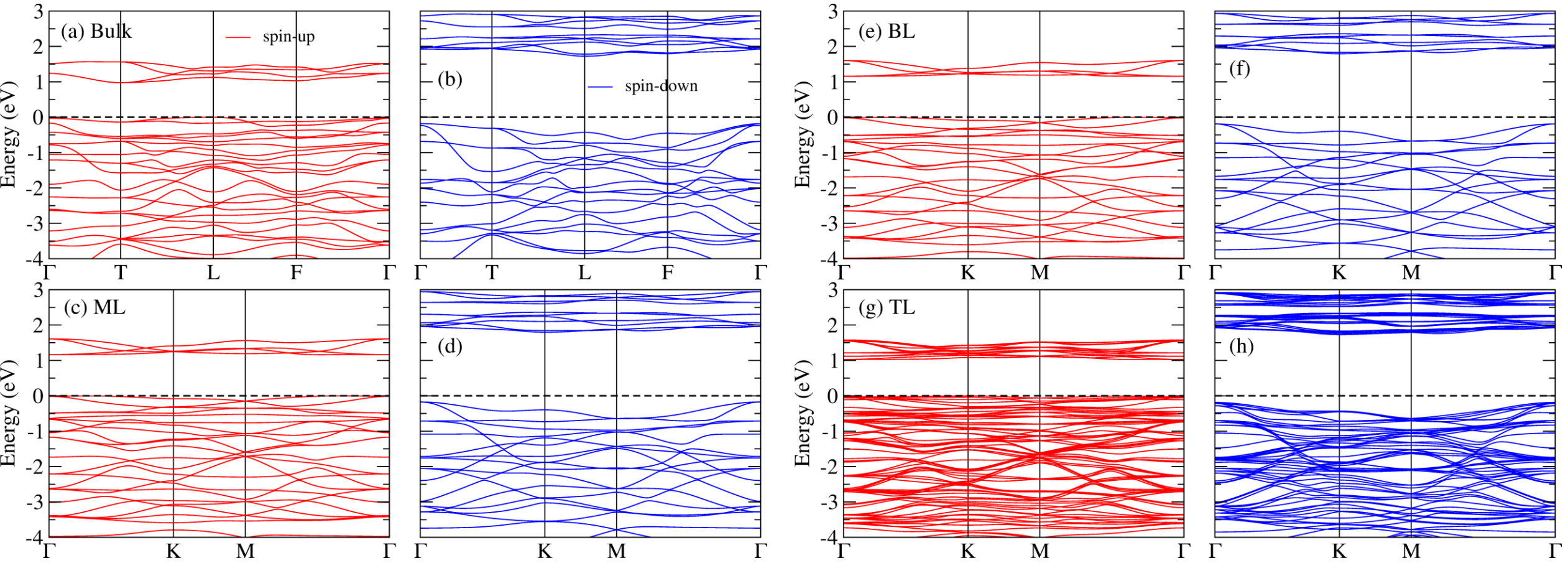


- The lower conduction bands and top valence bands of all the structures are of purely spin-up character
- This shows that all the structures are single-spin semiconductors and thus would be promising candidates for efficient spintronic and spin photovoltaic devices

# Spin-polarised density of states of $CrI_3$-Bulk:

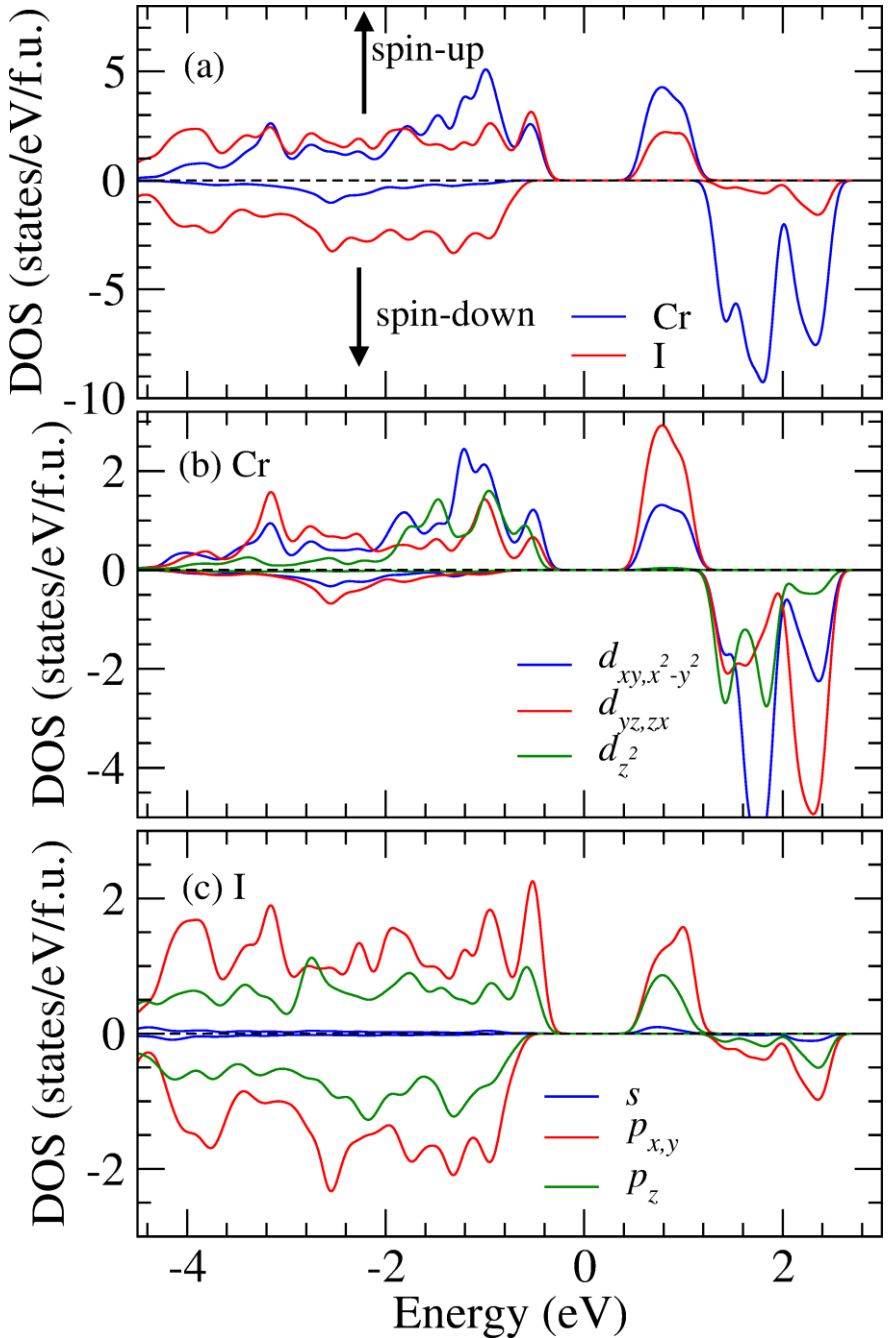


- The contributions to the valance and conduction bands mostly from the Cr-*d* orbitals with significant contributions from the I-*p* orbitals
- Contributions from both the Cr and I confirm the strong hybridization between Cr-*d* and I-*p* orbitals in $CrI_3$ structures
- The states in the upper valance band region of -4.3 eV to -0.3 eV are made up of spin-up Cr-$d_{xy,x^2-y^2}$ orbitals
- Conduction bands ranging from 0.4 eV to 1.2 eV is mainly because of spin-up Cr-$d_{xz,yz}$ orbitals
- The band gap in the $CrI_3$ structures arise due to the crystal-field splitting of spin-up Cr-$d_{xy,x^2-y^2}$ and $d_{xz,yz}$ bands
- Conversely, the DOS spectrum in spin-down valance band region are mostly contributed from I-*p* orbitals
- The spin-down conduction bands appear only above 1.3 eV with pronounced peaks of mainly Cr $d_{xy,x^2-y^2}$ and $d_{z^2}$ orbitals

# Spin-polarised density of states of $CrI_3$-ML:

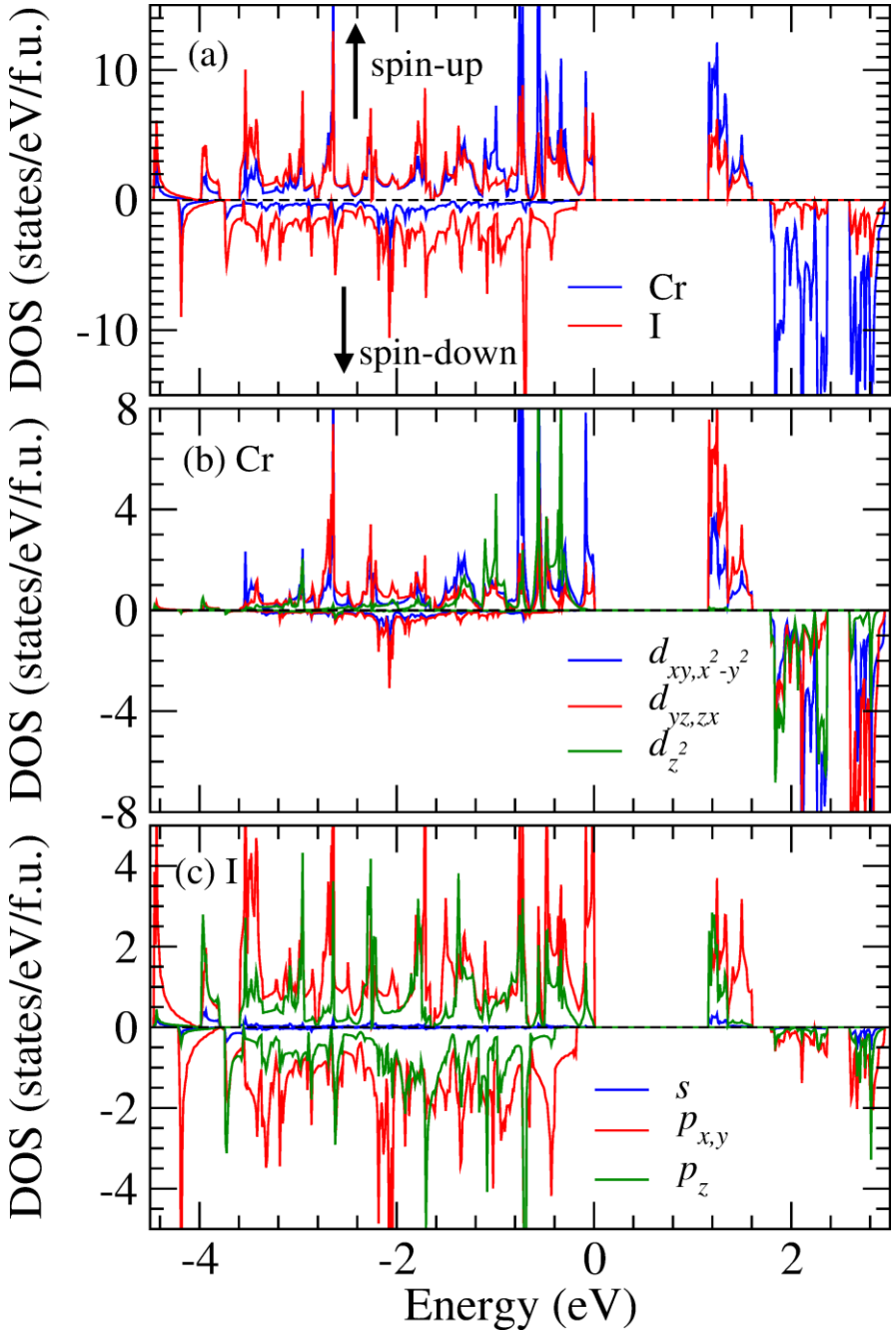


- The calculated total spin-up and spin-down DOS spectra of ML-$CrI_3$ are rather similar to that of bulk $CrI_3$
- The main difference comes from the contributions of the I-*p* orbital which is enhanced in the higher energy region in the ML
- A similar profile is observed in BL and TL structures

# Relativistic Band-structure: $CrI_3$-Bulk and multilayers

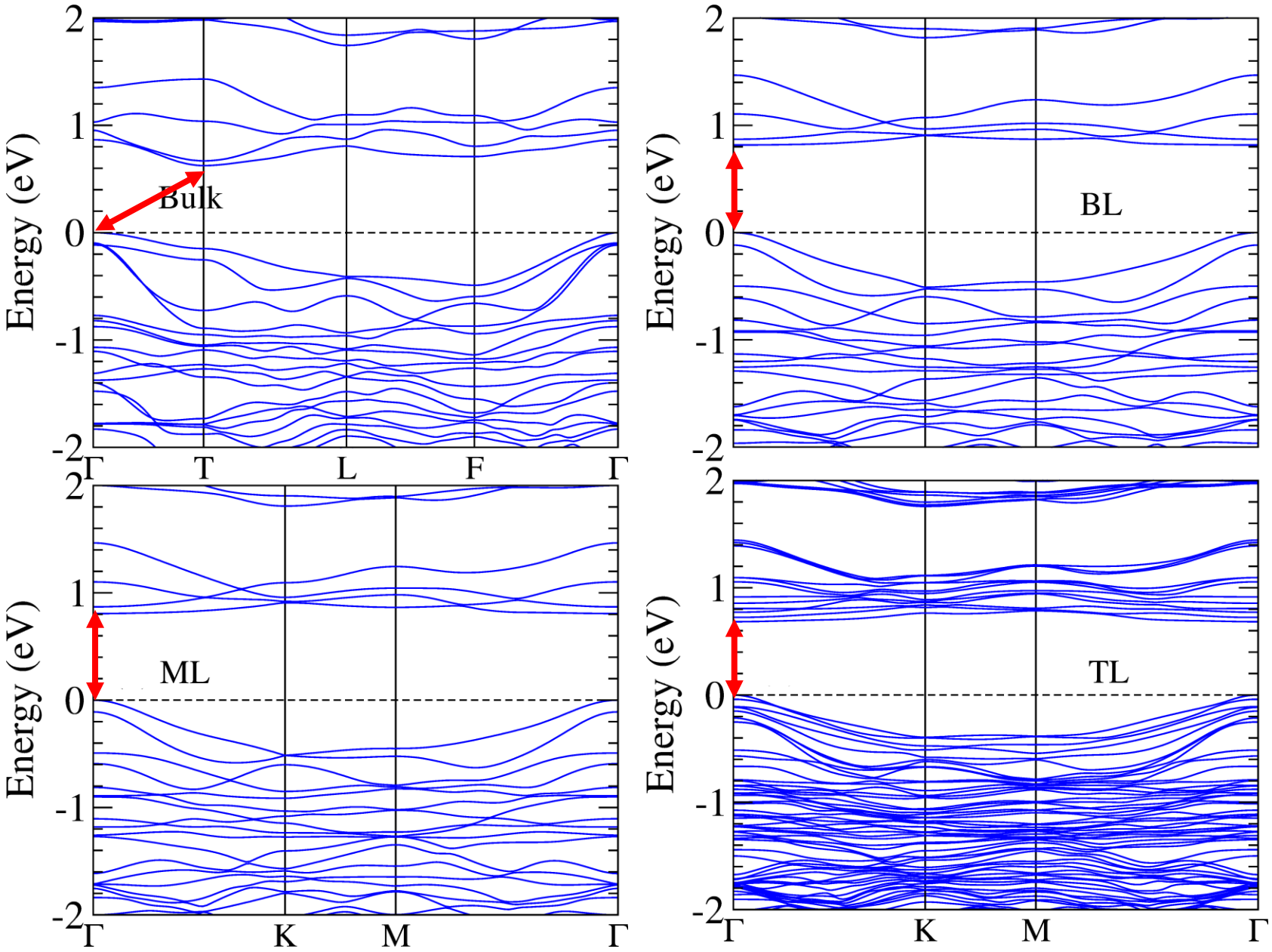


- Bulk $CrI_3$ show an indirect bandgap semiconductor whereas multi-layers shows the direct bandgap semiconducting nature
- In bulk, the valance band maximum (VBM) exist at Γ-point and the conduction band minimum (CBM) located at T point
- In case of multilayers VBM and CBM are exist at Γ-point, shows direct bandgap semiconducting nature

# Optical conductivity: $CrI_3$-bulk

- The optical conductivity elements for an in-plane electric polarization (E||ab) ($\sigma_{xx}$) differ significantly from that for the out-of-plane electric polarization (E||c) ($\sigma_{zz}$) above the absorption edge of about 1.5 eV
- The $\sigma^1_{xx} > \sigma^1_{zz}$ for bulk $CrI_3$ in the energy range from 1.5 to 4.4 eV, above this energy $\sigma^1_{xx} < \sigma^1_{zz}$
- This manifests that these structures are highly optically anisotropic
- Both Positive and Negative peak exits in real ($\sigma^1_{xy}$) and imaginary ($\sigma^2_{xy}$) parts of the off-diagonal optical conductivity elements, which is due to the inter-band transitions are dominated by left- or right-polarized-light (LCP and RCP) induced excitations
- $\sigma^1_{xy}$ shows a large positive peaks at 3.5 and 4.2 eV, $\sigma^2_{xy}$spectra shows at 4.8 eV for the bulk
- Negative peaks occurs in the vicinity of 1.3 eV in the $\sigma^1_{xy}$ spectrum and at 3.3 eV in the $\sigma^2_{xy}$ spectrum for bulk

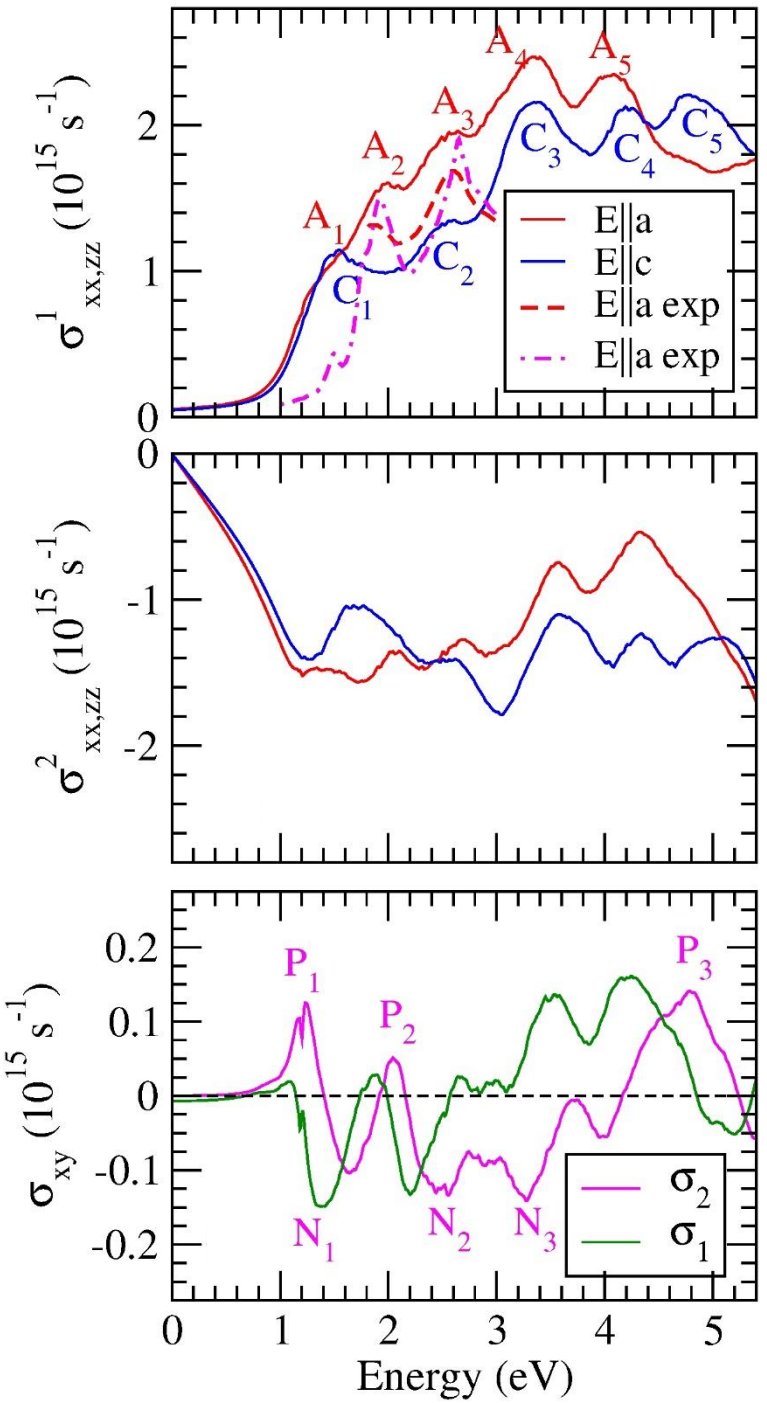

# Optical conductivity: ML $CrI_3$:

- A similar profile of bulk optical conductivity is observed in ML $CrI_3$ in the energy region of 1.0-4.3 eV, where $\sigma_{xx}^1 > \sigma_{zz}^1$, above 4.3 eV, $\sigma_{xx}^1 < \sigma_{zz}^1$
- The overall profile of the optical spectra in both bulk and ML are rather similar there exist a significant difference in $\sigma_{xx}$ and $\sigma_{zz}$, where, the difference among the E||ab and E||c found to be high compared to bulk structure

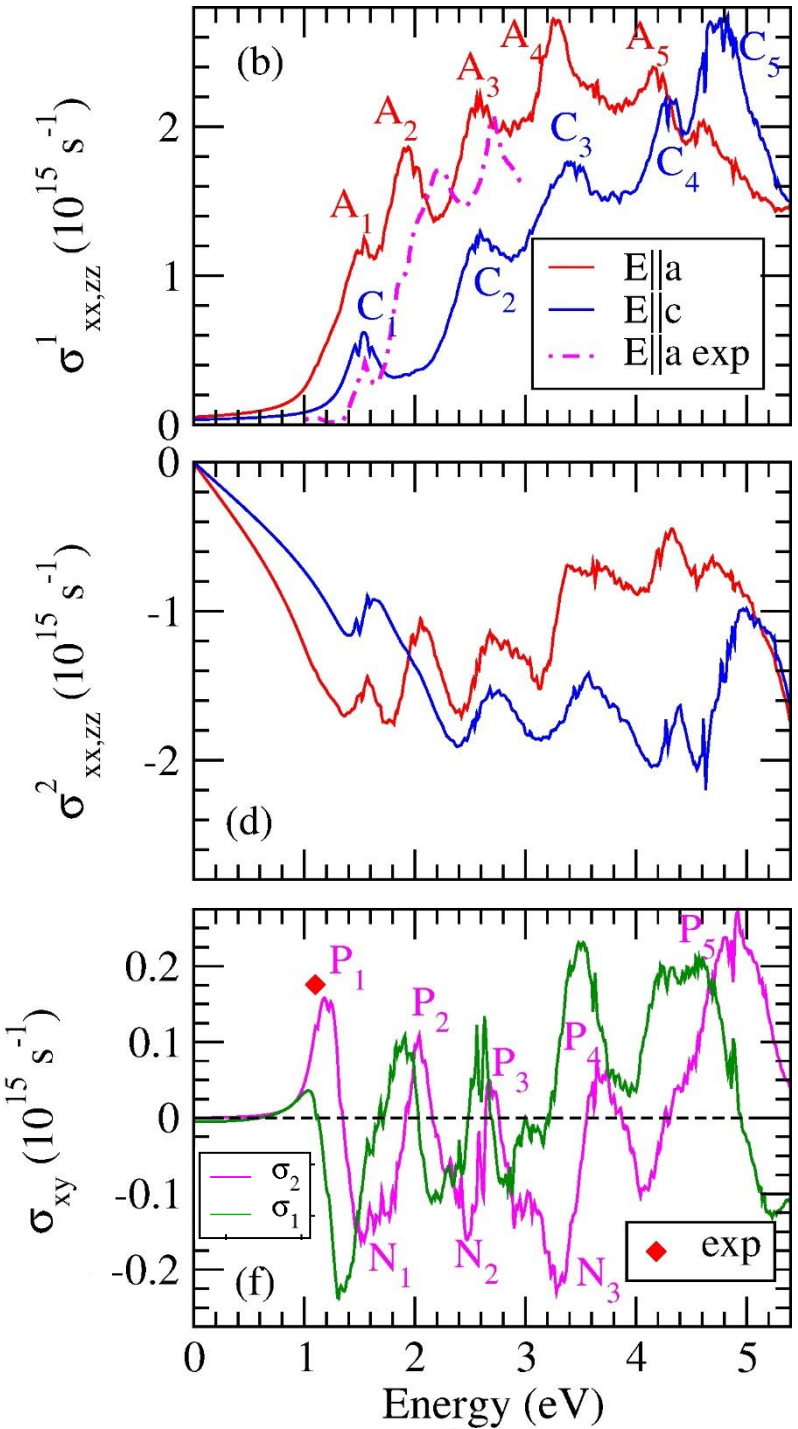

# Optical conductivity: $CrI_3$-BL and TL:

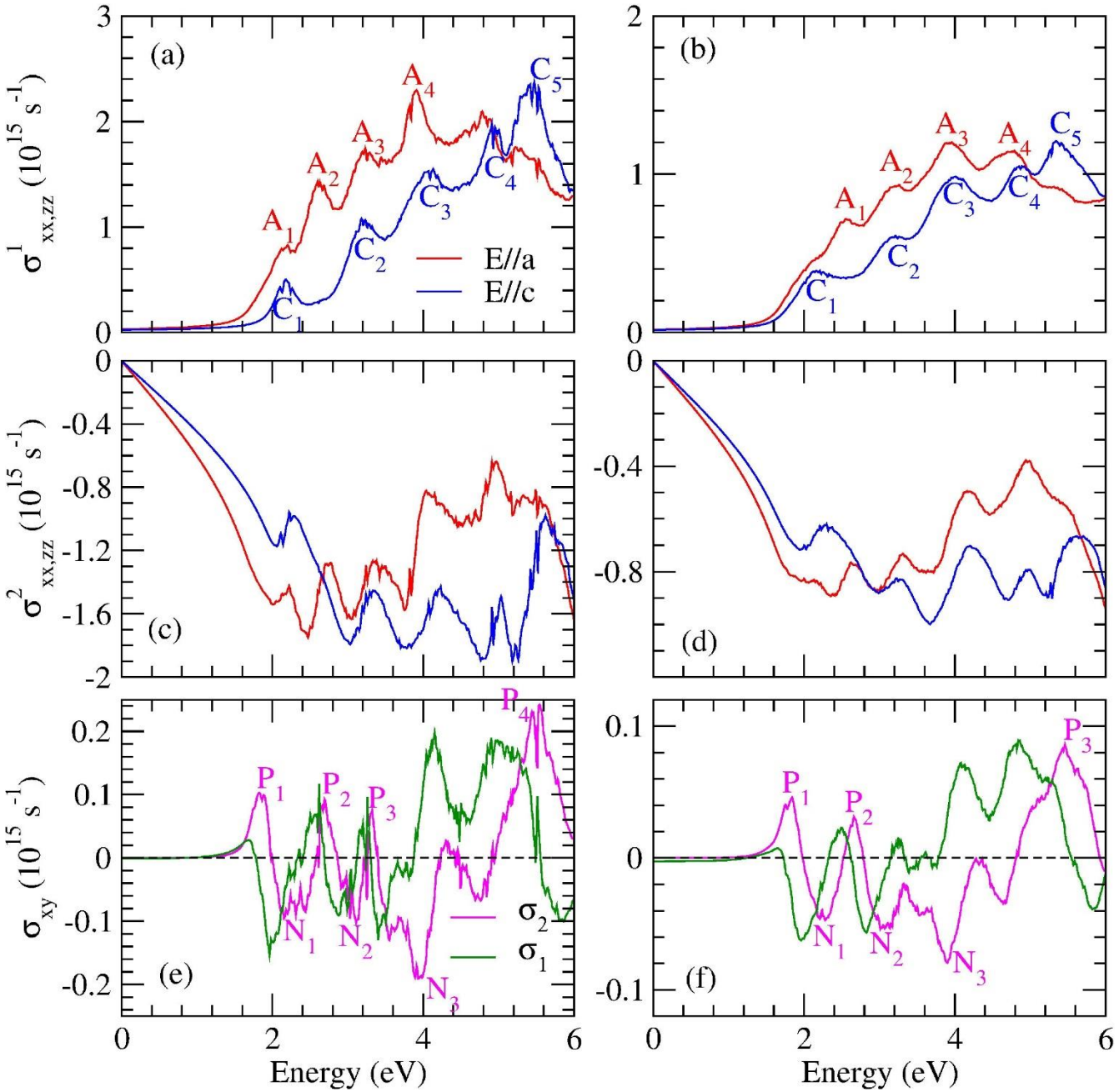


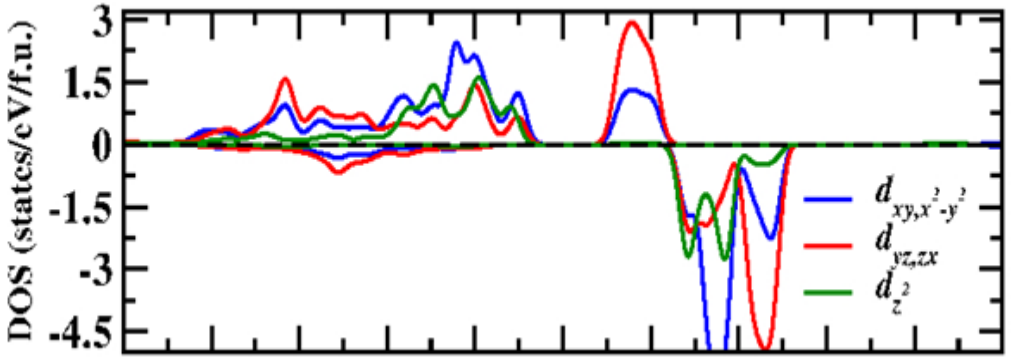


- A similar profile is observed in BL and TL structures, as that of ML
- The observed strong optical anisotropy is quite common in low dimensional materials and can be explained in terms of the orbital decomposed DOS
- As seen earlier from DOS, the upper valance band energy region of -4.5 to -0.3 eV, the dominate states are mainly from Cr-d $d_{xy,x^2-y^2}$ orbitals
- The $d_{xy,x^2-y^2}$ ($d_{z^2}$ ) states can be exited by only E⊥c (E||c) polarized light while Cr-$d_{xz,yz}$ orbitals can be exited by light of both polarization, this suggests $\sigma^1_{xx} > \sigma^1_{zz}$ in the low energy region up to 4.3 eV

# Optical conductivity: comparison with experiments

- Three peaks ($A_1$, $A_2$ and $A_3$) in the experimental differential reflection spectrum of bulk and ML $CrI_3$ agree very well with the theoretical ones in both shape and position, although the magnitude of the experimental spectrum is slightly smaller

- This indicates that our GGA+U calculations could describe the optical properties of $CrI_3$ quite well

- Assuming photoluminescence (PL) intensity (I) is proportional to photoabsorption (σ),

  PL circular polarization $\rho = \frac{I_+ - I_-}{I_+ + I_-} = \frac{\sigma_+^1 - \sigma_-^1}{\sigma_+^1 + \sigma_-^1} = \frac{\sigma_{xy}^2}{\sigma_{xx}^1}$

- $\sigma_{xy}^2 = \rho\sigma_{xx}^1$ estimated this way based on the calculated $\sigma_{xx}^1$ and experimental $\rho$ for ML $CrI_3$, which agree well with peak $P_1$ in the theoretical $\sigma_{xy}^2$ spectrum

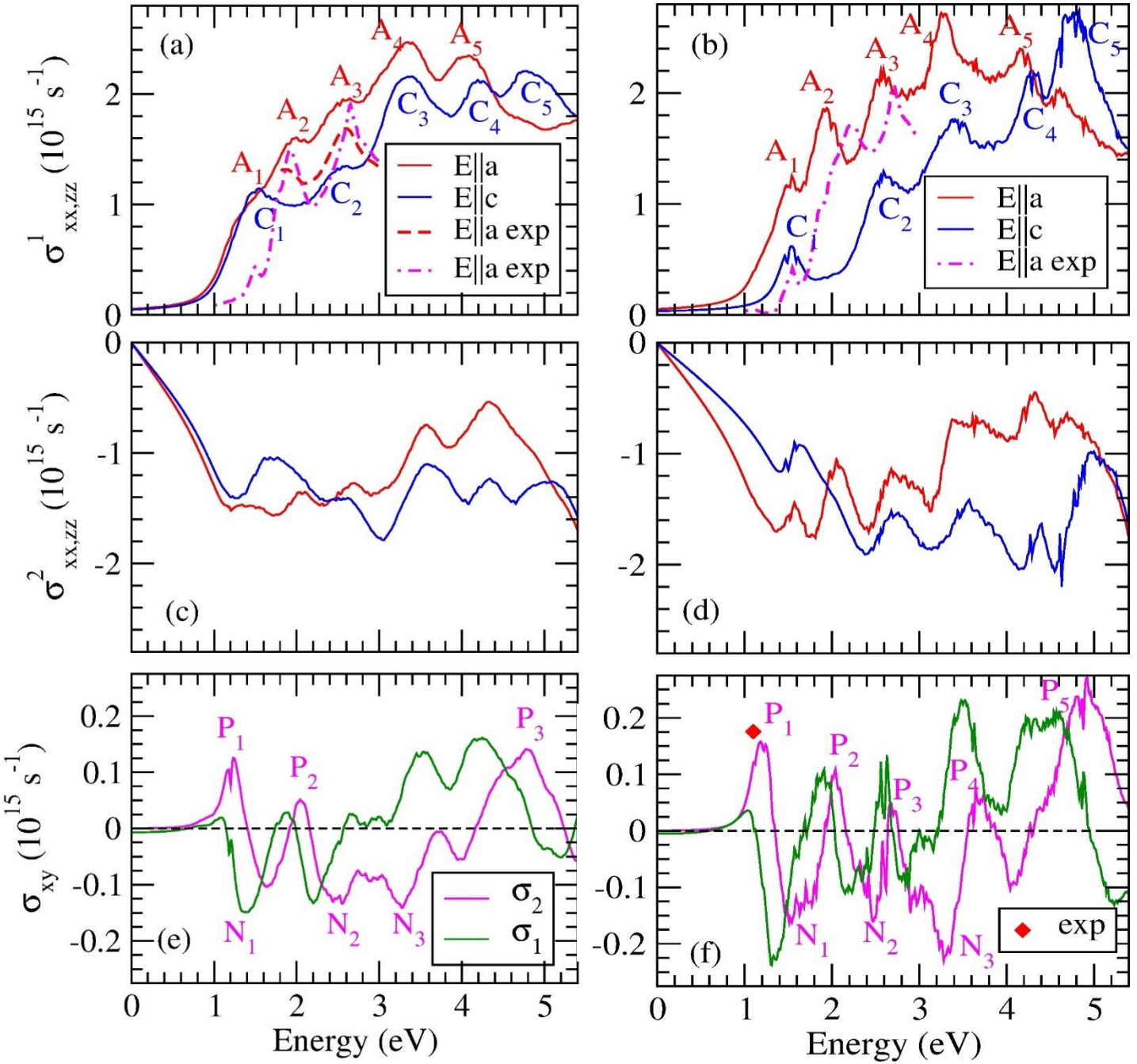


Gudelli et al, *New J. Phys.* **21** 053012 (2019)

# Magneto-optical Kerr effect:

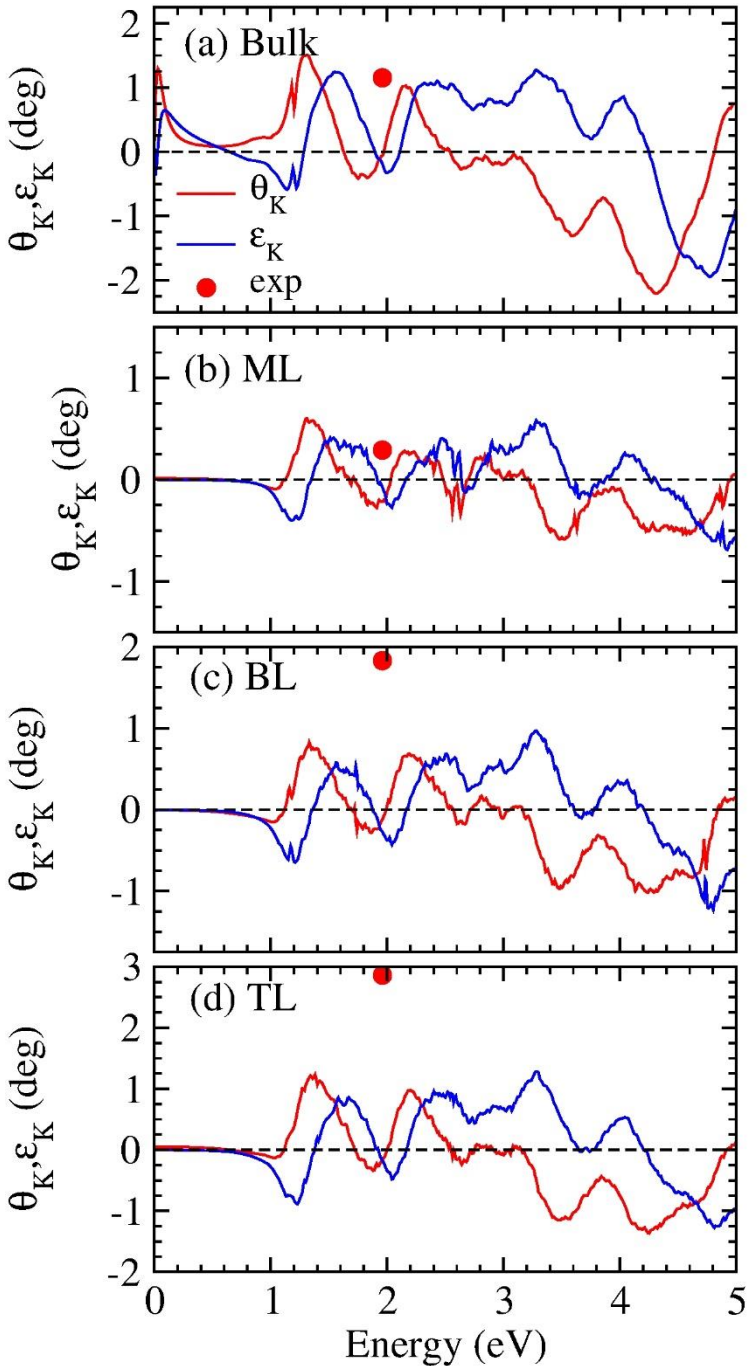


- Overall behaviour of the MO spectra for all the investigated structures is similar
- The $\theta_K^{max}$ angle occurs at 4.3 eV for the bulk (-2.1°) and at 4.2 eV for the TL (-1.3°), at 1.3 eV for the ML(0.6°) and 4.2 eV for the BL (-1.0°)
- Similarly, $\varepsilon_K^{max}$ near 4.8 eV for the bulk (-1.9°), at 3.3 eV for the ML(1.2°) and at 4.8 eV for BL (-1.2°) and TL (-1.3°)
- The measured and calculated $\theta_K$ values of bulk and ML $CrI_3$ would be in very good agreement, although the experimental $\theta_K$ values of BL and TL $CrI_3$ are much larger

3*d* transition metals: MnBi thin films, $\theta_K^{max}$ is 2.3° at 1.84 eV, for Pt based materials $\theta_K$ is 0.4-0.5° in FePt, $Co_2Pt$, and PtMnSb, which is due to the strong SOC of the Pt

3*d* transition semiconductor:

- $Ga_{1-x}Mn_xAs$ Kerr rotation angles of ~0.4° at 1.80 eV, $Y_3Fe_5O_{12}$ exhibits a significant Kerr rotation of 0.23° at 2.95 eV
- $Cr_2Ge_2Te_6$ has a $\theta_K$ value of ~0.14° for bulk, 0.0007° in BL, 0.002° in TL

Gudelli et al, *New J. Phys.* **21** 053012 (2019)

# Magneto-optical Faraday effect:

- $\theta_F^{max}$ exists at 4.3 eV for the bulk (-60°/μm) and the TL (-194°/μm), at 4.7 eV for the ML(-85°/μm) and the BL (-155°/μm)
- $\varepsilon_F^{max}$ near 4.8 eV for all the structures with 48°/μm, -85°/μm, -148°/μm and 170°/μm for the bulk, ML, BL and TL, respectively

- The measured Faraday rotation $\theta_F$ of bulk $CrI_3$ are almost in perfect agreement with our theoretical prediction

- MnBi films possess the largest $\theta_F$ angle of ~80 deg/μm, $Y_3Fe_5O_{12}$ show only 0.19 deg/μm at 2.07 eV, the replacement of Y with Bi has improved the $\theta_F$ by ~35 deg/μm at 2.76 eV making $Bi_3Fe_5O_{12}$ an outstanding MO material

- Clearly, in anyway the calculated Faraday rotation of the $CrI_3$ multilayers are comparable to that of prominent bulk MO metals

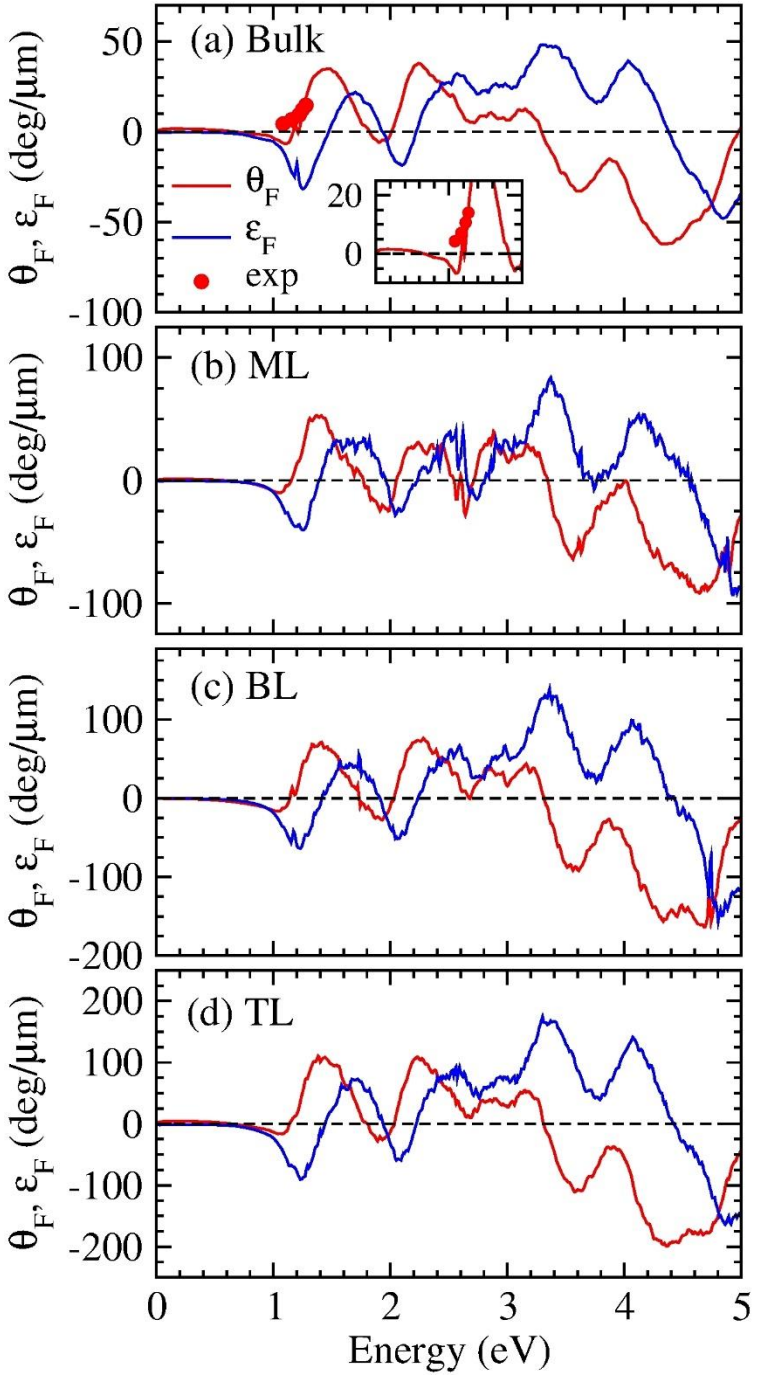


Ref: PRL 68, 3355 (1992); PRB 59, 15680 (1999); PRB 96, 167402 (2006)

# Conclusion:

- ✓ We find that both intralayer and interlayer magnetic couplings are strongly ferromagnetic in all the considered $CrI_3$ structures
- ✓ Ferromagnetic ordering temperatures estimated based on calculated exchange coupling parameters agree quite well with the measured ones
- ✓ All the structures have a large out-of-plane MAE of ~0.5 meV/Cr, these large MAEs suppress transverse spin fluctuations in atomically thin $CrI_3$ films and thus stabilize long-range magnetic orders at finite temperatures
- ✓ All the structures exhibit strong MO Kerr and Faraday effects, MO Kerr rotations up to ~2.6° are found, comparable to famous MO materials such as FM semiconductor $Y_3Fe_5O_{12}$ and metal PtMnSb
- ✓ Calculated MO Faraday rotation angles are also large, being up to ~200°/μm, and they are comparable to that of best known MO semiconductors such as $Y_3Fe_5O_{12}$ and $Bi_3Fe_5O_{12}$
- ✓ Calculated optical conductivity spectra, MO Kerr and Faraday rotation angles agree quite well with available experimental data
- ✓ Our findings of large out-of-plane MAEs and strong MO effects in these FM semiconducting $CrI_3$ ultrathin films suggest that they will find promising applications in high density semiconductor MO, low power spintronic nanodevices as well as efficient spin-photovoltaics

# Acknowledgements:


- Prof. Guo, Guang-Yu, National Taiwan University and NCTS, Taiwan
- Physics Division, NCTS

# Thank You !!!